Effect of Heavy Metals on Dechlorination of Carbon Tetrachloride by Iron Nanoparticles

Hsing-Lung Lien,* Yu-Sheng Jhuo, and Li-Hua Chen

Department of Civil and Environmental Engineering
National University of Kaohsiung
Kaohsiung 811, Taiwan, Republic of China

ABSTRACT

Effects of heavy metals on the dechlorination of carbon tetrachloride by iron nanoparticles were investigated in terms of reaction kinetics and product distribution using batch systems. Removal of heavy metals and the interaction between heavy metals and iron nanoparticles at the iron surface were also examined. It was found that Cu(II) enhanced the carbon tetrachloride dechlorination by iron nanoparticles and led to produce more benign products (i.e., CH_4). Pb(II) may increase reduction rate slightly but also increase the production of more toxic intermediates such as dichloromethane. In comparison to the iron reduction system without heavy metals, effects of As(V) were negligible while Cr(VI) decreased the dechlorination rate by a factor of 2. Removal of As(V) by iron nanoparticles behaved pseudo-first-order reaction kinetics but a fast initial removal followed by a slow subsequent process was found in the cases of Cu(II) and Pb(II). Scanning electron microscopy-energy dispersive X-ray (SEM-EDX) analysis indicated the deposition of heavy metals onto the iron surface. X-ray diffraction (XRD) analysis showed Cu(II) was reduced to metallic copper and cuprite (Cu_2O) at the iron surface while no reduced lead species was observed from the Pb(II)-treated iron nanoparticles. Limited data suggested an oxidized lead species formed. The enhanced dechlorination by Cu(II) can be attributed to the deposition of metallic copper and cuprite at the iron surface. This study suggests that implementation of iron nanoparticles rather than engineered bimetallic iron nanoparticles for remediation of mixed contamination with both chlorinated organics and heavy metals is sufficient.

Key words: arsenic; lead; copper; chlorinated methane; reduction; groundwater

INTRODUCTION

**C**HLORINATED ORGANIC SOLVENTS and heavy metals are two common classes of contaminants often detected in contaminated subsurface. Chlorinated organic solvents such as tetrachloroethylene and trichloroethylene have been in widespread use for several decades in industrial applications including the manufacture of herbicides, plastics, and solvents (Rammamoorthy and Rammamoorthy, 1997). Many of them had been listed as prior-

*Corresponding author: Department of Civil and Environmental Engineering, National University of Kaohsiung, No. 700, Kaohsiung University Rd., Kaohsiung 811, Taiwan, Republic of China. *Phone:* +886-7591-9221; *Fax:* +886-7591-9376; *E-mail:* lien.sam@nuk.edu.tw.

ity pollutants by the U.S. Environmental Protection Agency (U.S. EPA). On the other hand, increasingly higher quantities of heavy metals are being released into the environment through anthropogenic activities, primarily associated with industrial processes, manufacturing, and disposal of industrial and domestic refuse and waste materials (U.S. EPA, 1997).

Remediation of contaminated groundwater using iron nanoparticles has been developed (Wang and Zhang, 1997). Iron nanoparticles with a diameter less than 100 nm can be delivered into hot spot through a direct injection technology (Zhang, 2003; Schrick *et al.*, 2004). Iron nanoparticles are capable of treating a wide variety of contaminants including chlorinated organic solvents (Lien and Zhang, 1999, 2001), heavy metals (Kanel *et al.*, 2005; Yuan and Lien, 2006), and other inorganic contaminants (e.g., perchlorate) (Cao *et al.*, 2005).

Engineered bimetallic iron nanoparticles have widely been reported for improving the performance of monometallic iron nanoparticles (Schrick *et al.*, 2002; Feng and Lim, 2005). Engineered bimetallic iron nanoparticles (e.g., Pd/Fe, Ni/Fe) can be synthesized by chemical reduction and precipitation.

$$M^{2+} + Fe^0 \rightarrow M^0 + Fe^{2+} \ (M^{2+}$$
$$= e.g., \ Pd^{2+}, \ Ni^{2+}) \quad (1)$$
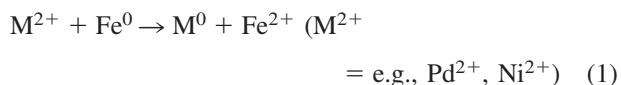
The deposition of a small amount of a second metal at the iron surface increased reaction rates significantly. For example, surface area-normalized reactivity of bimetallic Pd/Fe nanoparticles is one to two orders of magnitude higher than that of iron nanoparticles (Lien and Zhang, 2001). Iron serves as an effective electron donor while the enhancement of reduction rates has been attributed to (1) catalytic effects of second metals (e.g., Pd) through hydrogen reduction rather than direct electron transfer (Li and Farrell, 2000), (2) a galvanic corrosion leading to the increase of corrosion rates (Zhang *et al.*, 1998), and (3) the prevention of an oxide formation at the iron surface (Schrick *et al.*, 2002).

It is not an unusual case that the mixed contamination of heavy metals and chlorinated solvents occurs at the same site (Puls *et al.*, 1999). The presence of heavy metals in contaminated sites could be capable of serving as the source of second metals resulting in the *in situ* formation of bimetallic iron nanoparticles when monometallic iron nanoparticles were implemented. Treatments of mixed contaminants containing both chlorinated organic compounds and toxic metals using reactive iron have recently received attention (Jeong and Hayes, 2003; Dries *et al.*, 2005). In this study, we focused on the effect of heavy metals on the influence of performance for iron nanoparticles in reacting with carbon tetrachloride. Heavy metals including As(V),

Cu(II), and Pb(II) were investigated systematically. Interface reaction between heavy metals and iron was examined by X-ray diffraction (XRD) and scanning electron microscopy-energy dispersive X-ray (SEM-EDX) analysis. Hexavalent chromium, Cr(VI), was also selected to test its effect on the iron-mediated dechlorination.

MATERIALS AND METHODS

Chemicals

All chemicals were reagent grade or above and used without further purification. Deionized water was used for preparation of all reagent solutions. Sodium arsenate 7-hydrate ($Na_2HAsO_4 \cdot 7H_2O$, 99%), copper (II) sulphate ($CuSO_4$, 99%) and lead (II) acetate trihydrate (($CH_3COO)_2Pb \cdot 3H_2O$, 99+%) were purchased from J. T. Baker (Phillipsburg, NJ), Sigma (St. Louis, MO), and Aldrich (Milwaukee, WI), respectively. Sodium borohydride (NaBH4, 98%) and ferric chloride ($FeCl_3 \cdot 6H_2O$, 98%) were obtained from Aldrich. Carbon tetrachloride (99.5%) was purchased from SHOWA (Showa Chemical Co., Tokyo, Japan). Chloroform (99%) and dichloromethane (99.9%) were obtained from J.T. Baker. A standard gas mixture for GC analysis was obtained from Supelco (Bellefonte, PA), which contained 1% each of ethane, ethylene, acetylene, and methane.

Synthesis of iron nanoparticles

Synthesis of iron nanoparticles was achieved by adding 1:1 volume ratio of $NaBH_4$ (0.25 M) into $FeCl_3 \cdot 6H_2O$ (0.045 M) solution. The borohydride to ferric iron ratio was 7.4 times higher than that of the stoichiometric requirement [Equation (2)]. Excessive borohydride was applied to accelerate the synthesis reaction and ensure uniform growth of iron crystals. Ferric iron was reduced by borohydride according to the following reaction:

$$4Fe^{3+} + 3BH_4^- + 9H_2O \rightarrow 4Fe^0$$
$$+ 3H_2BO_3^- + 12H^+ + 6H_2 \quad (2)$$
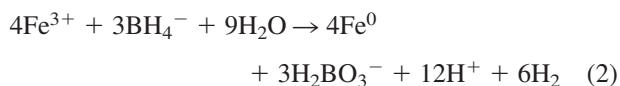
The suspension was mixed vigorously under room temperature (22 ± 1°C). The iron particles were then washed with large volume (>1,000 mL/g iron) of Milli-Q water for at least three times and were used without further treatments unless indicated otherwise.

Batch tests

For the study of heavy metal removal, experiments were carried out in a 250-mL high-density poly(ethylene), (HDPE), vessel containing 2.5 g/L iron nanoparticles in 100 mL of metal ion solution at 22 ± 1°C. Stock solutions of 1,000 mg/L metal ions were prepared from

reagent-grade chemicals in deionized water. Initial concentrations of metal ions were 25 mg/L corresponding to 1 wt% of iron content in the batch tests. Reaction vessels were placed on a rotary shaker (50 rpm). The solution pH was controlled only at the beginning of the reaction and adjusted to at pH 7.0 ± 0.2. The experiments were conducted in duplicate to check the reproducibility of batch results. Acceptable variability for duplicate batch runs agrees within 10%.

For the study of carbon tetrachloride degradation, batch experiments were conducted in 150-mL serum bottles (Wheaton, Millville, NJ; actual volume was approximately 162 mL). For each batch bottle, 20-μL methanol solution of carbon tetrachloride was spiked into a 100-mL aqueous solution. In a typical experiment, the initial concentration of carbon tetrachloride and individual metal ion was 30 and 25 mg/L, respectively. The metal loading of iron nanoparticles was 2.5 g/L. The serum bottles were then capped with a Teflon-faced septum and aluminum crimp cap and mixed on a rotary shaker (50 rpm) at room temperature (22 ± 1°C). Control tests without iron nanoparticles were conducted with identical experimental conditions and initial concentrations of reactants. Analyses of organic mass in the controls indicated that the mass varied by less than 5% over the course of a typical experiment. The experiments were conducted in triplicate. Acceptable variability for triplicate batch runs agrees within 15%.

Method of analyses

Analysis of heavy metals was carried out using an inductively coupled plasma-optical emission spectrometry (ICP-OES, Perkin-Elmer Optima 2000DV; Perkin-Elmer Inc., Norwalk, CT). The wavelength of As(V), Cu(II), and Pb(II) was set at 193.7, 324.8, and 220.4 nm, respectively. Prior to analysis, samples were filtered through 0.2-μm filters and acidified with 3% HNO_3. Analyses of duplicate samples indicated a relatively analytical error of less than 5% for metal concentration analyzed in the laboratory.

Concentrations of carbon tetrachloride and its intermediates were measured by a headspace-gas chromatograph (GC) method. At selected time intervals, a 50-μL headspace gas aliquot was withdrawn by a gastight syringe for GC analysis. Headspace samples were analyzed by a HP4890 GC-FID equipped with a DB-624 capillary column (30 m × 0.32 mm) (J&W Scientific, Santa Clara, CA). Temperature conditions were programmed as follows: oven temperature at 45°C for 5 min, injection port temperature at 250°C, and detector temperature at 300°C. Concentrations of hydrocarbons were measured by a HP4890 GC-FID equipped with a GS-GASPRO capillary column (J&W, 30 m × 0.32 mm). Temperature conditions were programmed as follows: oven temperature at 35°C for 5 min, injection port temperature at 200°C; and detector temperature at 300°C. Concentrations of chlorinated methanes and hydrocarbons were determined by the external standard method using calibration curves. Calibration curves for each compound were made initially and the variability was checked daily before analysis (<15%).

Solid-phase characterization

Characterization of iron nanoparticles was conducted using X-ray diffraction (XRD), scanning electron microscopy (SEM), and a surface area analyzer. XRD measurements were performed using a X-ray diffractometer (Siemens D5000) with a copper target tube radiation (Cu K_α) producing X-ray with a wavelength of 1.54056 Å. Samples were placed on a quartz plate and were scanned from 20° to 80° (2θ) at a rate of 2° 2θ/min. Morphological analysis of iron nanoparticles was performed by SEM using a Hitachi S-4300 microscope (Hitachi High-Tech Science Systems Corp., Ibaraki, Japan) with energy-dispersive X-ray (EDX) analysis (at 10 kV). The specific surface area of iron nanoparticles was measured by Brunauer-Emmett-Teller (BET) N_2 method using a COULTER SA 3100 surface are analyzer (Coulter Co., Miami, FL). Analysis of the specific surface area of iron nanoparticles was conducted in triplicate.

Reaction kinetics

The reaction rate of both organic and inorganic contaminant removal was determined with pseudo first-order reaction kinetics:

$$\frac{dC}{dt} = -k_a C \qquad (3)$$

where C is the concentration of contaminants in the aqueous phase (mg/L); k_a is the observed first-order rate constant (h^{-1}); and t is time (h).

RESULTS AND DISCUSSION

Characterization of iron nanoparticles

Figure 1 shows the SEM image of iron nanoparticles that are comprised of spherical particles assembled in chains. The average diameter of iron nanoparticles was in the range of 50–100 nm. The size of particles is consistent with previous studies and the observation of chain structure of iron nanoparticles is in agreement of the study conducted by Nurmi *et al.* (2005). A specific surface area of iron nanoparticles was in an average of 33.5 ± 4.2 m²/g as measured by BET surface analyzer.
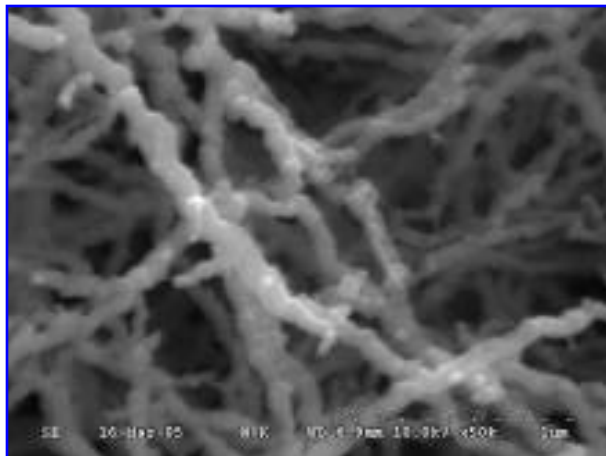
Figure 1. SEM image of the fresh iron nanoparticles.

Removal of heavy metals by iron nanoparticles

Removal of Cu (II), Pb(II), and As(V) by iron nanoparticles is shown in Fig. 2. Initial concentration of heavy metals was 25 mg/L, and the dose of iron was 2.5 g/L. The removal of As(V) can be fitted well by pseudo-first-order reaction kinetics [Equation (3)]. The observed rate constant was 0.94 h^{-1} ($R^2 = 0.99$) corresponding to a surface-area normalized rate constant (k_{SA}) of 11.2 mL/h/m^2. This is a substantially high As(V) removal rate for elevated level of arsenic compared to that obtained from most microsized iron particles at lower arsenic concentrations (Su and Puls, 2001). However, a fast initial removal followed by a slow subsequent process was found in the case of both Cu(II) and Pb(II). Disappearance of more than 93% of total Cu(II) and Pb(II) occurred within 5 min. The first order reaction kinetics was simply not fitted with the data. This result is consistent with studies conducted by Ponder *et al.* (2000). They suggested a physical mechanism was involved in this type of removal processes. Overall, the different removal behavior among As(V), Cu(II), and Pb(II) suggests that the removal of these heavy metals involves different mechanisms.

The disappearance of metal ions in the aqueous solution was attributed to the deposition at iron nanoparticle surface confirmed by SEM-EDX analysis. To ensure the deposition of heavy metals onto the iron surface, the concentration of heavy metals conducted in surface analysis was 10 times higher than that used in batch kinetic experiments. Samples were taken when iron nanoparticles
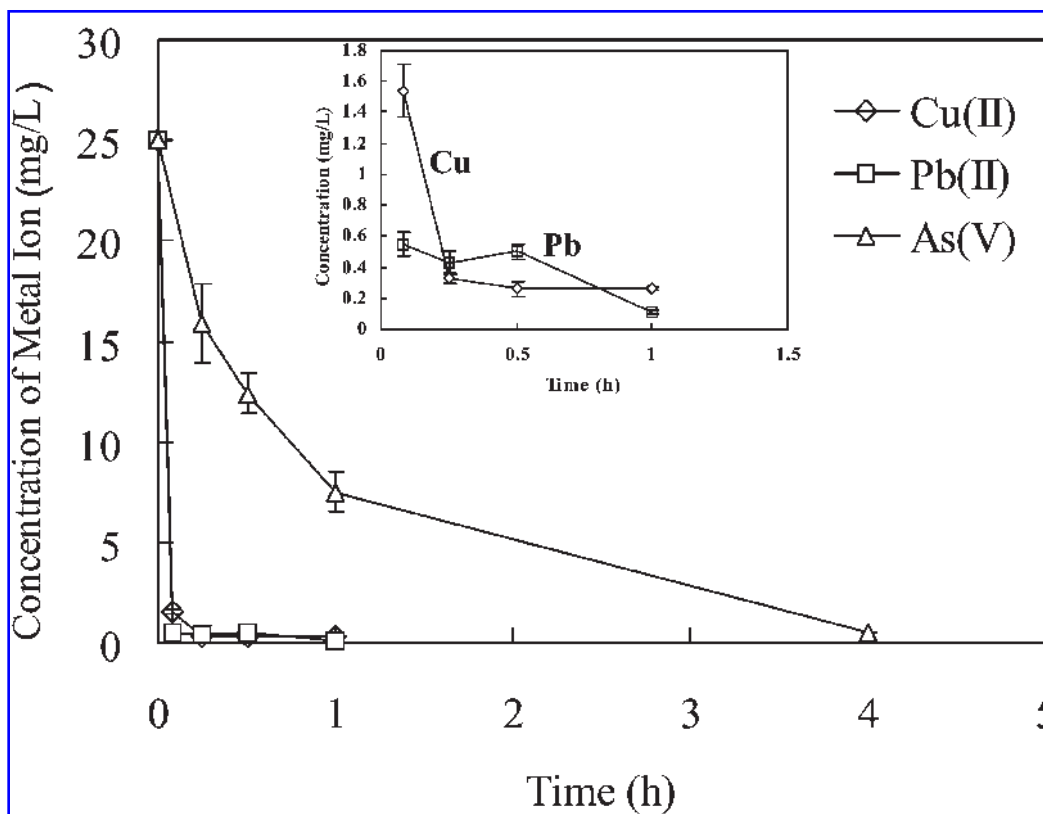

Figure 2. Removal of heavy metals by iron nanoparticles. Initial concentration of metal ions was 25 mg/L and the dose of iron nanoparticles was 2.5 g/L. Insert shows the concentration change of Cu (II) and Pb(II) at a lower level.

reacted with 250 mg/L of metal ions for a day. As shown in Fig. 3, the EDX spectra indicated the existence of arsenic, copper, and lead at the surface of reacted iron nanoparticles.

XRD analysis was further conducted to better understand the interaction between heavy metals and iron at the nanoparticle surface. The XRD analysis of fresh iron nanoparticles shows two major characteristic peaks at $44.8°$ and $65.2°$ degrees 2θ, indicating the presence of elemental iron (Fig. 4A). A small amount of iron oxide (maghemite and/or magnetite) appeared in the fresh sample. This could be attributed to a short exposure to air during the transport of fresh iron nanoparticles into a vessel before they were dried by nitrogen overnight.

Figure 4B shows the XRD pattern for Cu(II)-treated iron nanoparticles taken after reacting with 250 mg/L Cu(II) for 12 h. Iron corrosion products (magnetite and/or maghemite) were found at the surface. Removal of Cu(II)
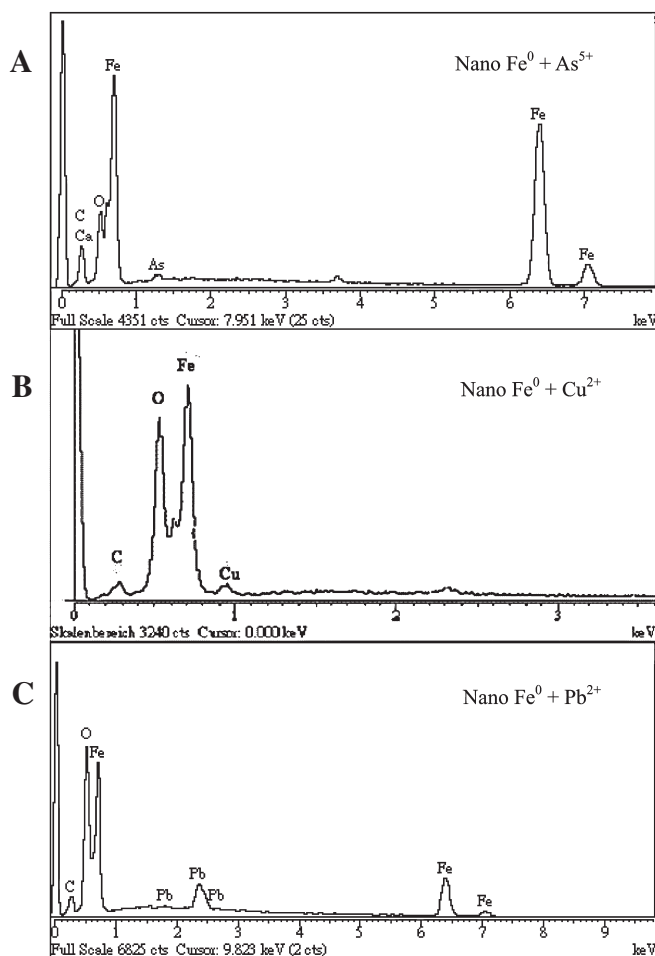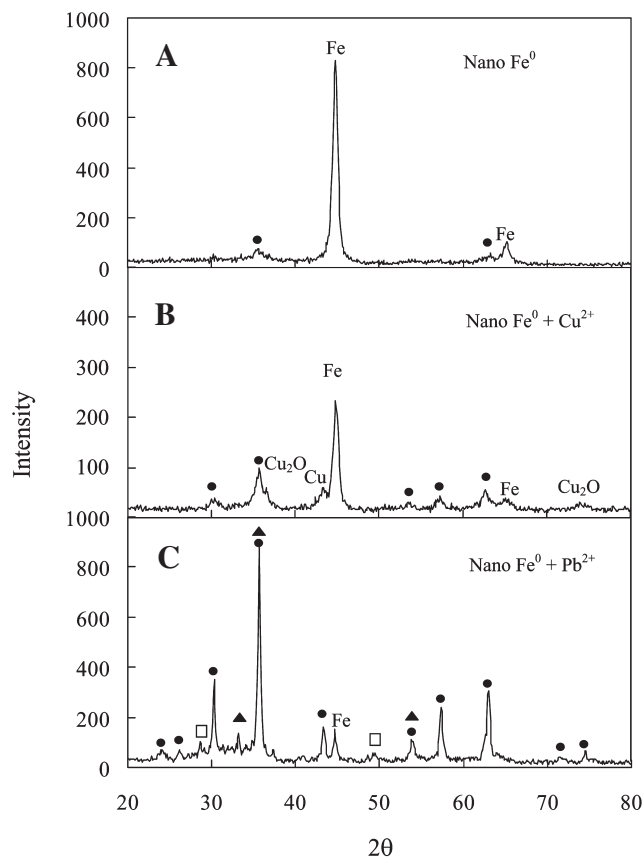
Figure 4. XRD patterns of (**A**) fresh, (**B**) Cu(II)-treated iron nanoparticles, and (**C**) Pb(II)-treated iron nanoparticles. Peaks are due to zero-valent iron (Fe), metallic copper (Cu), cuprite (Cu_2O), magnetite/maghemite ($Fe_3O_4/\gamma\text{-}Fe_2O_3$) (●), and hematite ($Fe_2O_3$) (▲). Peaks assigned to $\alpha\text{-}PbO_2$ are indicated by an open square symbol (□).

Figure 3. SEM-EDX spectra of heavy metal-treated iron nanoparticles: (**A**) As(V), (**B**) Cu(II), and (**C**) Pb(II).

by iron nanoparticles involved the formation of two copper species, metallic copper (Cu^0) and cuprite (Cu_2O), that were identified at the iron surface. Because the standard reduction potential of Cu^{2+}/Cu^0 and $Fe^{2+}/Fe0$ couples is $+0.34$ and -0.44 V, respectively (Table 1), metallic copper can be formed through the redox reaction:

$$Cu^{2+} + Fe^0 \rightarrow Cu^0 + Fe^{2+} \qquad (4)$$
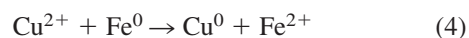
The overall E° for this reaction ($E°_{rxn}$) is $+0.78$ V at 25°C, indicating a strongly favorable reaction from a thermodynamics perspective. As indicated in Fig. 2 that the removal of Cu(II) by iron nanoparticles is a very fast reaction, Equation (4) actually represents a synthetic step for making engineered bimetallic particles (e.g., Pd/Fe, Cu/Al, Ni/Fe) (Grittini *et al.*, 1995; Fennelly and Roberts, 1998; Kim and Carraway, 2000; Lien and Zhang, 2002). The formation of Cu_2O could be attributed to the reac-

Table 1. The standard reduction potential of varius heavy metals (Lide, 1993).

Species	Reaction	Standard reduction potential (V)
Fe^{2+}	$Fe^{2+} + 2e^- \rightarrow Fe^0$	−0.447
Cu^{2+}	$Cu^{2+} + 2e^- \rightarrow Cu^0$	+0.3419
Pb^{2+}	$Pb^{2+} + 2e^- \rightarrow Pb^0$	−0.1262
As^{5+}	$AsO_4^{3-} + 4H_2O + 5e^- \rightarrow As^0 + 8OH^-$	−1.39
Cr^{6+}	$Cr_2O_7^{2-} + 14H^+ + 6e^- \rightarrow 2Cr^{3+} + 7H_2O$	+1.232
Cr^{3+}	$CrO_2^- + 2H_2O + 3e^- \rightarrow Cr^0 + 4OH^-$	−1.2

tion between Fe(II) and Cu(II) in the aqueous solution (Maithreepala and Doong, 2004):

$$2Fe^{2+} + 2Cu^{2+} + 7H_2O \rightarrow Cu_2O$$
$$+ 2Fe(OH)_3 + 8H^+ \quad (5)$$
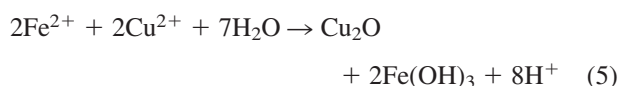
The XRD pattern for Pb(II)-treated iron nanoparticles taken after reacting with 250 mg/L Pb(II) for 24 h is shown in Fig. 4C. Iron corrosion products including hematite and magnetite and/or maghemite were detected. Theoretically, the reduction of Pb(II) to metallic lead should be thermodynamically favorable in the presence of zero-valent iron ($E^o_{rxn} = +0.32$ V, Table 1). However, neither Pb^0 nor Pb(II) oxides (e.g., PbO, Pb(OH)$_2$) were identified in the sample, which was inconsistent with the study conducted by Ponder *et al.* (2000). After carefully examining the XRD pattern, it was found that two minor peaks at 28.6° and 49.4° 2θ, which had a relative intensity of 11.4 and 6.4%, respectively, matched scrutinyite (α-PbO$_2$: 28.6°, 49.4°, and 32.7° 2θ). It is unusual to observe no Pb^0 but Pb(IV) species in an iron reduction system. No observation of Pb^0 might be due to low deposition amounts of Pb^0 that was unable to be detected by XRD. Although the evidence to support the formation of Pb(IV) species is very limited in this study, the possibility should not be ruled out. Recently, oxidation of As(III) to As(V) has widely been reported in the zero-valent iron system (Su and Puls, 2004; Kanel *et al.*, 2005; Lien and Wilkin, 2005). It has been found that the zero-valent iron has the capacity for oxidation in the presence of oxygen, possibly through the formation of hydroxide radials (Joo *et al.*, 2005). In addition, the reductive activation of dioxygen is another possible process for the oxidation of contaminants by zero-valent metals (Lien and Wilkin, 2002). In this study, batch reactors were sealed under ambient conditions without purging with nitrogen. The oxygen in the reaction system may be a factor and further investigation is needed.

The XRD analysis for As(V)-treated iron nanoparticles exhibited only iron oxide species such as maghemite and/or magnetite (data not shown) and no crystal phases of arsenic species deposited at the iron surface was found. Reduction of As(V) to metallic arsenic (As^0) is unlikely (Melitas *et al.*, 2002) because such reaction is thermodynamically unfavorable under ambient conditions ($E^o_{rxn} = -0.94$ V, Table 1). However, as shown in Fig. 3, EDX analysis indicated the deposition of arsenic at the iron surface suggesting the removal of As(V) with iron nanoparticles was a complicated process that could involve surface adsorption, precipitation, and coprecipitation (Nikolaidis *et al.*, 2003).

Dechlorination of carbon tetrachloride by iron nanoparticles in the presence of heavy metals

Figure 5A shows the carbon tetrachloride degradation with iron nanoparticles in the absence of heavy metals. Approximately 96% of carbon tetrachloride was dechlorinated and produced several intermediates. Chloroform appeared as the major byproduct accounting for 40% of the carbon tetrachloride lost. The yield of dichloro-methane and methane was about 19 and 14%, respectively. Trace amounts (<2% in total) of hydrocarbon such as ethane, ethylene, and acetylene were detected. Observed rate constant was determined to be about 0.13 h^{-1} ($R^2 = 0.98$).

In the presence of Cu(II), an increase of carbon tetrachloride degradation rate was found (Fig. 5B). Approximately 96% of carbon tetrachloride was degraded within 12 h. Chloroform (41%) peaked at 2 h and gradually decreased. Methane appeared immediately after carbon tetrachloride was added to the aqueous solution and continued to accumulate after the disappearance of carbon tetrachloride.

Figure 5C shows the dechlorination of carbon tetrachloride by iron nanoparticles in the aqueous solution containing with 25 mg/L of Pb(II). Dechlorination rate was slightly increased by the existence of Pb(II) and, again, chloroform, dichloromethane, and methane were observed. However, unlike the results shown in Fig. 5A and B, dichloromethane (47%) became the major product in this test. Both chloroform (23%) and methane (8%) accumulated relatively steady during the course of the reaction.
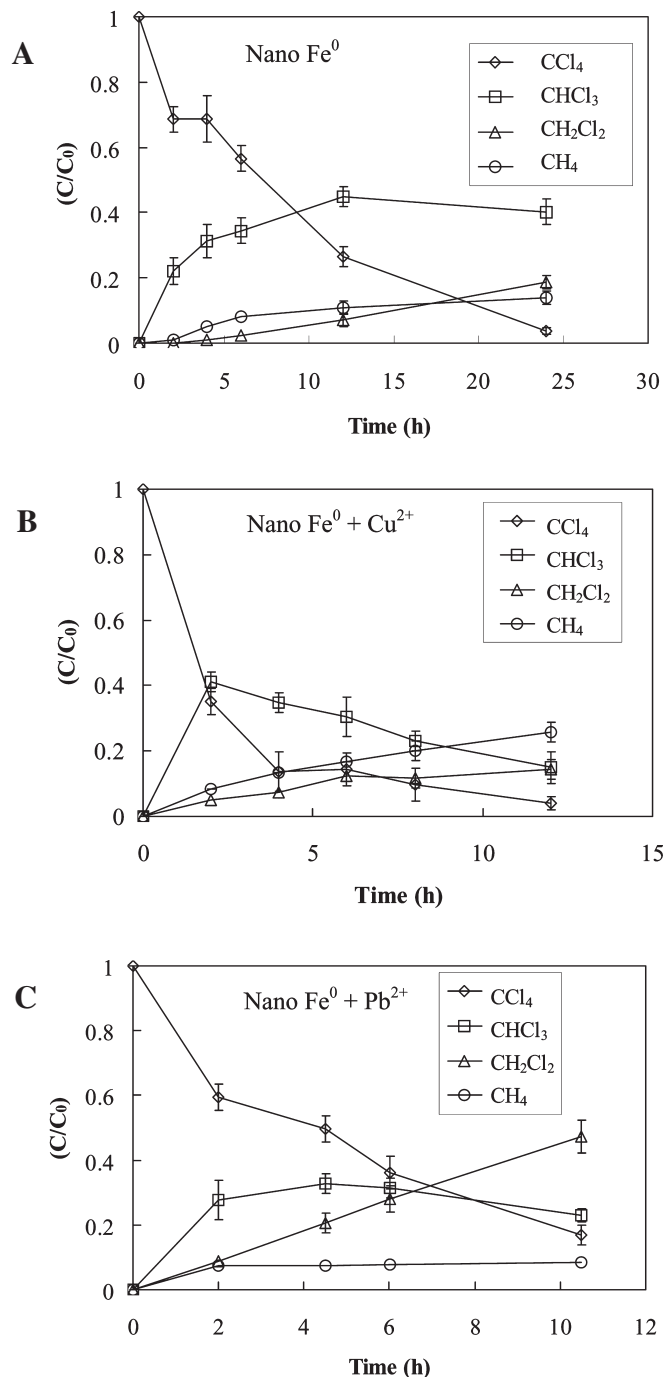
Figure 5. Dechlorination of carbon tetrachloride by iron nanoparticles. (**A**) in the absence of heavy metals, (**B**) in the presence of Cu(II), and (**C**) in the presence of Pb(II).

Effects of heavy metals on carbon tetrachloride dechlorination

Effects of heavy metals on the degradation of carbon tetrachloride in terms of reaction rates and product dis-

tribution are shown in Figs. 6 and 7, respectively. Dechlorination of carbon tetrachloride followed pseudo first-order reaction kinetics, which had R^2 values between 0.91 and 0.98. It was found that both Cu(II), and Pb(II) enhanced the dechlorination rate of carbon tetrachloride by iron nanoparticles while the effect of As(V) on the carbon tetrachloride dechlorination was negligible (Fig. 6). Among them, Cu(II) exhibited the best promoting effect, which increased the dechlorination rate by a factor of 2 compared to the reaction system with iron nanoparticles alone. It is worthy of note that Cr(VI) decreased the degradation rate of carbon tetrachloride by iron nanoparticles. In comparison to the iron reduction system in the absence of heavy metals, dechlorination of carbon tetrachloride was two times slower in the presence of 25 mg/L of Cr(VI). This is consistent with previous studies (Schlicker *et al.*, 2000; Dries J. *et al.*, 2005) suggesting a competitive effect between the strong oxidant Cr(VI) and carbon tetrachloride in reaction with zero-valent iron. Although Cr(VI) is readily reduced to Cr(III) (E^o_{rxn} = +1.68 V, Table 1), Cr(III) cannot be reduced to Cr^0 (E^o_{rxn} = −0.75 V, Table 1). Therefore, the formation of bimetallic Cr/Fe structure onto the iron surface is unlikely.

Figure 7 shows the product distribution from the carbon tetrachloride degradation by iron nanoparticles with various heavy metals. The concentration of carbon tetrachloride and its products were measured when reactions completed during a period of 24 h. It was found that individual heavy metals had distinctive effects on the product distribution of carbon tetrachloride dechlorination. In the presence of Cu(II), significant amounts of methane (34%) and less amounts of chloroform (8%) were produced, although incomplete recovery of carbon still ac-
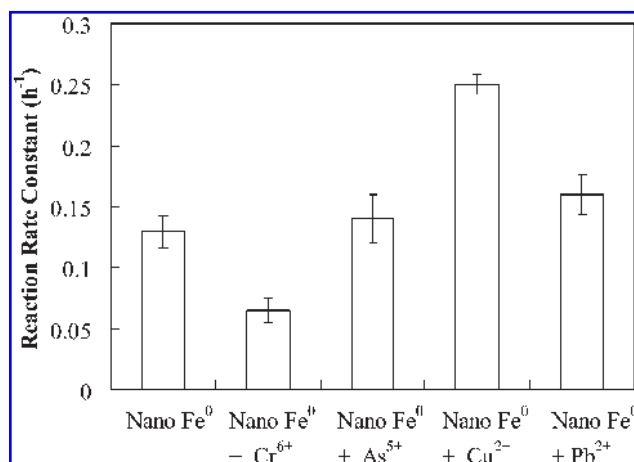

Figure 6. Effects of heavy metals on rates of the carbon tetraachloride dechlorination by iron nanoparticles.
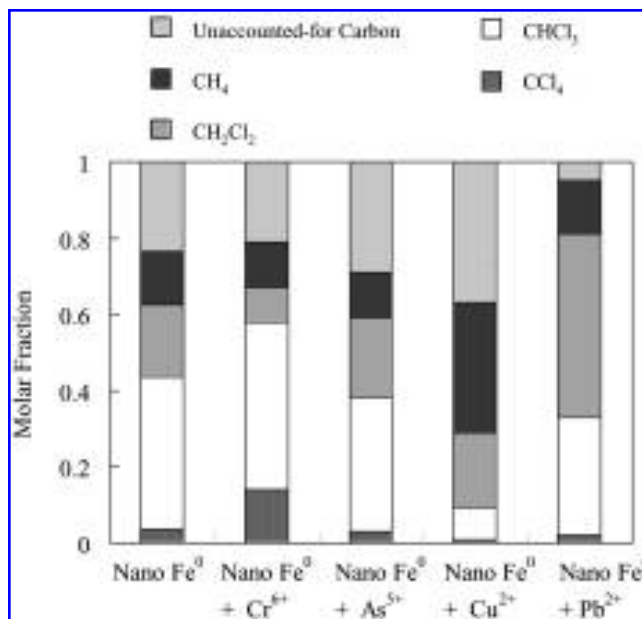
Figure 7. Effects of heavy metals on the product distribution for the carbon tetrachloride dechlorination by iron nanoparticles.

counted for about 40%. However, the presence of Pb(II) led to the accumulation of dichloromethane (48%). There was no significant difference between the reaction system with iron nanoparticle alone and that with both iron nanoparticles and As(V) for the product distribution. Unlike the above-mentioned metals, Cr(VI) decelerated degradation rates and resulted in a relatively large amount of carbon tetrachloride remaining unreacted (14%). It also caused the accumulation of chloroform (44%) in the reaction system.

Because methane is relatively benign, whereas dichloromethane is more toxic than carbon tetrachloride, the presence of Cu(II) in the iron reduction system exhibited a positive effect on the degradation of carbon tetrachloride. Although Pb(II) may enhance the dechlorination rate, the accumulation of significant amounts of dichloromethane limited the benefit of Pb(II) in the iron reduction system.

The enhanced dechlorination of carbon tetrachloride by iron nanoparticles with Cu(II) can be attributed to the formation of bimetallic structure. The XRD analysis indicated metallic copper was deposited at the iron surface (Fig. 4b). The bimetallic structure leads a galvanic corrosion taking place readily at the surface to facilitate the electron transfer for the surface-mediated dechlorination of carbon tetrachloride. Moreover, metallic copper is known as a mild hydrogenation catalyst (Satterfield, 1991). It is effective for most of the elementary reactions that are required in catalytic dehalogenation (Yang *et al.*, 1997). Studies have demonstrated bimetallic Cu/Fe accelerate reduction rates (Fennelly and Roberts, 1998; Kim and Carraway, 2000). In

addition, the formation of Cu_2O at the iron surface may serve as a reductant beneficial to the carbon tetrachloride degradation (Maithreepala and Doong, 2004).

Implication to in situ *remediation*

Considering the frequent occurrence of both chlorinated organic solvents and heavy metals, the development of technologies for treatment of mixed contaminants at the same site is necessary. The iron nanoparticle has shown its potential for treating both types of contaminants. In this study, we demonstrated that iron nanoparticles can form bimetallic iron nanoparticles in the presence of certain heavy metals such as Cu(II) that resulted in increasing dechlorination rates and producing more benign products. Because Cu(II) is an inorganic contaminant commonly found at a contaminated site, the remediation of chlorinated organic solvents using iron nanoparticles rather than engineered bimetallic iron nanoparticles may be sufficient. However, heavy metals such as Cr(VI) and Pb(II) may cause negative effects that decreased reaction rates and/or produced more toxic intermediates. Careful examination of the effects of heavy metals is necessary before implementation of iron nanoparticles for remediation of mixed contamination.

ACKNOWLEDGMENTS

REFERENCES

CAO, J., ELLIOTT, D.W., and ZHANG, W-X. (2005). Perchlorate reduction by nanoscale iron particle. *J. Nanoparticle Res.* **7,** 499.

DRIES, J., BASTIAENS, L., SPRINGAEL, D., AGATHOS, S.N., and DIELS, L. (2005). Combined removal of chlorinated ethenes and heavy metals by zerovalent iron in batch and continuous flow column systems. *Environ. Sci. Technol.* **39,** 8460.

FENNELLY, J.P., and ROBERTS, A.L. (1998). Reaction of 1,1,1-trichloroethane with zero-valent metals and bimetallic reductants. *Environ. Sci. Technol.* **32,** 1980.

FENG, J., and LIM, T. (2005). Pathways and kinetics of carbon tetrachloride and chloroform reductions by nano-scale Fe and Fe/Ni particles: Comparison with commercial micro-scale Fe and Zn. *Chemosphere* **59,** 1267.

GRITTINI, C., MALCOMSON, M., FERNANDO, Q., and KORTE, N. (1995). Rapid dechlorination of polychlorinated biphenyls on the surface of a Pd/Fe bimetallic system. *Environ. Sci. Technol.* **29,** 2898.

JEONG, H.Y., and HAYES, K.F. (2003). Impact of transition metals on reductive dechlorination rate of hexachloroethane by mackinawite. *Environ. Sci. Technol.* **37,** 4650.

JOO, S.H., FEITZ, A.J., SEDLAK, D.L., and WAITE, T.D. (2005). Quantification of the oxidizing capability of nanoparticulate zero-valent iron. *Environ. Sci. Technol.* **9,** 1263.

KANEL, S.R., MANNING, B., CHARLET. L., and CHOI, H. (2005). Removal of arsenic(III) from groundwater by nanoscale zero-valent iron. *Environ. Sci. Technol.* **39,** 1290.

KIM, Y., and CARRAWAY, E.R. (2000). Dechlorination of pentachlorophenol by zero valent iron and modified zero valent irons. *Environ. Sci. Technol.* **34,** 2014.

LI, T., and FARRELL, J. (2000). Reductive dechlorination of trichloroethene and carbon tetrachloride using iron and palladized-iron cathodes. *Environ. Sci. Technol.* **34,** 173.

LIDE, D.R. Editor-in-chief (1993–1994). *Handbook of Chemistry and Physics*, 74th ed. Boca Raton, FL: CRC Press.

LIEN, H.-L., and WILKIN, R.T. (2002). Reductive activation of dioxygen for degradation of methyl *tert*-butyl ether by bifunctional aluminum. *Environ. Sci. Technol.* **36,** 4436.

LIEN, H.-L., and ZHANG, W.-X. (1999). Dechlorination of chlorinated methanes in aqueous solutions using nanoscale bimetallic particles. *J. Environ. Eng.* **125,** 1042.

LIEN, H.-L., and ZHANG, W.-X. (2001). Iron nanoparticles for complete reduction of chlorinated ethenes. *Colloids Surfaces A: Physicochem. Eng. Aspects* **191,** 97.

LIEN, H.-L., and ZHANG, W.-X. (2002). Enhanced dehalogenation of halogenated methanes by bimetallic Cu/Al. *Chemosphere* **49,** 371.

LIEN, H.-L., and WILKIN, R.T. (2005). High-level arsenite removal from groundwater by zero-valent iron. *Chemosphere* **59,** 377.

MAITHREEPALA, R.A., and DOONG, R. (2004). Synergistic effect of copper ion on the reductive dechlorination of carbon tetrachloride by surface-bound Fe(II) associated with goethite. *Environ. Sci. Technol.* **38,** 260.

MELITAS, N., CONKLIN, M., and FARRELL, J. (2002). Electrochemical study of arsenate and water reduction on iron media used for arsenic removal from potable water. *Environ. Sci. Technol.* **36,** 3188.

NIKOLAIDIS, N.P., DOBBS, G.M., and LACKOVIC, J.A. (2003). Arsenic removal by zero-valent iron: Field, laboratory and modeling studies. *Water Res.* **37,** 1417.

NURMI, J.T., TRATNYEK, P.G., SARATHY, V., BAER, D.R., AMONETTE, J.E., PECHER, K., WANG, C., LINEHAN, J.C., MATSON, D.W., PENN, R.L., *et al.* (2005). Characterization and properties of metallic iron nanoparticles: Spectroscopy, electrochemistry, and kinetics. *Environ. Sci. Technol.* **39,** 1221.

PONDER, S.M., DARAB, J.G., and MALLOUK, T.E. (2000). Remediation of Cr(VI) and Pb(II) aqueous solution using supported nanoscale zero-valent iron. *Environ. Sci. Technol.* **34,** 2564.

PULS, R.W., BLOWES, D.W., and GILLHAM, R.W. (1999). Long-term performance monitoring for a permeable reactive barrier at the U.S. Coast Guard Support Center, Elizabeth City, North Carolina. *J. Hazard. Mater.* **68,** 109.

RAMMAMOORTHY, S., and RAMMAMOORTHY, S. (1997). *Chlorinated Organic Compounds in the Environment: Regulatory and Monitoring Assessment.* Boca Raton, FL: CRC Press.

SATTERFIELD, C.N. (1991). *Heterogeneous Catalysis in Industrial Practice*, 2nd ed. New York: McGraw-Hill Inc.

SCHLICKER, Q., ERBERT, M., FRUTH, M., WEIDNER, M. WÜST, W., and DAHMKE, A. (2000). Degradation of TCE with iron: The role of competing chromate and nitrate reduction. *Ground Waster* **38,** 403.

SCHRICK, B., BLOUGH, J.L. JONES, A.D., and MALLOUK, T.E. (2002). Hydrodechlorination of trichloroethylene to hydrocarbons using bimetallic nickel-iron nanoparticles. *Chem. Mater.* **14,** 5140.

SCHRICK, B., HYDUTSKY, B.W., BLOUGH, J.L., and MALLOUK, T.E. (2004). Delivery vehicles for zerovalent metal nanoparticles in soil and groundwater. *Chem. Mater.* **16,** 2187.

SU, C., and PULS, R.W. (2001). Arsenate and arsenite removal by zerovalent iron: Kinetics, redox transformation, and implications for in situ groundwater remediation. *Environ. Sci. Technol.* **35,** 1487.

SU, C., and PULS, R.W. (2004). Significance of iron(II,III) hydroxycarbonate green rust in arsenic remediation using zerovalent iron in laboratory column test. *Environ. Sci. Technol.* **38,** 5224.

U.S. Environmental Protection Agency. (1997). *Technology Alternatives for the Remediation of Soils Contaminated with As, Cd, Cr, Hg, and Pb.* EPA/540/S-97/500. Edison, NJ: Office of Research and Development (ORD), National Risk Management Research Laboratory (NRMRL).

WANG, C., and ZHANG, W.-X. (1997). Nanoscale metal particles for dechlorination of TCE and PCBs. *Environ. Sci. Technol.* **31,** 2154.

YANG, M.X., SARKAR, S., and BENT, B.E. (1997). Degradation of multiply-chlorinated hydrocarbons on Cu(100). *Langmuir* **13,** 229.

YUAN, C., and LIEN, H.-L. (2006). Removal of arsenate from aqueous solution using nanoscale iron particles. *Water Qual. Res. J. Can.* **41**(2), 210.

ZHANG, W.-X. (2003). Iron nanoparticles for environmental remediation: An overview. *J. Nanoparticle Res.* **5,** 323.

ZHANG, W.-X., WANG, C., and LIEN, H.-L. (1998). Treatment of chlorinated organic contaminants with nanoscale bimetallic particles. *Catal. Today* **40,** 387.